Erbium Doped Cobalt Nano-Ferrites: Preparation and Structural Properties.

Edapalli Sumalatha
Osmania University
D Ravinder (ravindergupta28@rediffmail.com)
Osmania University https://orcid.org/0000-0002-0626-3034
N.V.Krishna Prasad
GITAM University - Bengaluru Campus
Khalid Mujasam Batoo
King Saud University
Emad H. Raslan
King Saud University
Muhammad Hadi
King Saud University

Original Research

Keywords: Cobalt-Erbium nano-ferrites, XRD, TEM

Posted Date: February 9th, 2021

DOI: https://doi.org/10.21203/rs.3.rs-175790/v1

Erbium Doped Cobalt Nano-Ferrites : Preparation and structural Properties.

Edapalli Sumalatha[1], D. Ravinder[1*],N.V.Krishna Prasad[2], Khalid Mujasam Batoo[3], Emad H. Raslan[4] and Muhammad Hadi[4]

[1]Department of Physics, Osmania University, Hyderabad-500007, Telangana, India
[3]Department of Physics, GITAM Deemed to be University, Bangalore, Karnataka-562163, India
[3]King Abdullah Institute for Nanotechnology, King Saud University, P.O. Box-2455, Riyadh-11451, Saudi Arabia.
[4]Department of Physics, College of Science,King Saud University, P.O. Box-2455, Riyadh-11451, Saudi Arabia.

***Corresponding Author Email ID: ravindergupta28@rediffmail.com**

Abstract:

Synthesized nano-ferrits of Cobalt-Erbium having chemical formula $CoEr_xFe_{2-x}O_4$(x= 0 to 0.030 with step size 0.05) were characterized using X-Ray Diffraction (XRD) and Transmission Electron Microscopy (TEM). Structural variables that include lattice constant (a), crystallite size (D), X-ray density (dx) and surface area (s) were computed from XRD patterns. XRD patterns confirmed single phase cubic spinal structure while TEM results revealed homogeneous nature of particles accompanied by clusters without impurity peaks. The observed results are explained on the basis of composition.

Keywords: Cobalt-Erbium nano-ferrites, XRD, TEM

1.Introduction:

Healthy research has been accomplished on fundamental, technological and potential applications of nano-ferrites. Nanomaterials of spinel ferrite find several applications in technology that include high density magnetic information storage devices [1], ferrofluid technology[2], magneto caloric refrigeration[3], magnetic diagnostics and drug delivery[4], magnetic recording media and magnetostriction [5], magnetic sensors, microwave devices and electrical generators etc. Ferrites are insulators exhibiting various magnetic and electric properties such as low electrical conductivity, dielectric loss, magnetic loss, relative loss factor,

moderate dielectric constant, high initial permeability and saturation magnetization. Doping and thermal changes during synthesis and processing of cobalt-ferrites alter the distribution of metal ions influencing their structure and magnetic properties [6]. It is reported that the net magnetic moment of lanthanide series elements/ions depend on f-orbital electron number in which Er^{+3} is of small size (89 pm) with large magnetic moment (7 μB) [7]. Low eddy current and high resistivity makes ferrites better choice than metals [8]. The present work reports the preparation and characterization of erbium doped cobalt ferrites using Citrate-gel auto combustion.

2. Experimental Procedure:

2.1. Synthesis of Cobalt-Erbium nano-ferrites with citrate-gel auto combustion technique

Cobalt Nitrate (Co(NO3)2·6H2O), Ferric Nitrate (Fe(NO3)3·9H2O), Erbium Nitrate (Er (NO3).6H2O), Citric Acid (C6H8O7·H2O) and Ammonia solution (NH3) of 99.9% purity weighed as per stoichiometric ratio were used as starting materials. Liquefaction of metal nitrates in distilled water was done and the mixture was stirred at 300 rpm for one hour to obtain a clear homogeneous solution. Next citric acid in aqueous form and metal nitrate was maintained in 1:3 ratio for all samples. Now, ammonia solution was added drop by drop to maintain Ph=7. This solution on stirring was heated at 100 °C temperature for ten to twelve hours to form a viscous gel. The water contained in the mixture gets evaporated slowly to form dry gel generating internal combustion to form a black colored sample. This sample was manually grinded and calcinated at 500°C for four hours. Later these samples in pellet or powder form are characterized with XRD (Bruker, CuKα,λ = 0.15406nm) and TEM (Model JEOL2100F,Japan).

3.1. XRD Analysis of Co-Er nano-ferrites:

Figure.1 depicts the XRD pattern of Co-Er nano-ferrites which indicated single-phase cubic spinel structure without any impurity peak. Figure.2 displays the Rietveld Refinement corresponding to $CoEr_xFe_{2-x}O_4$ samples with x value between 0.00 to 0.030 (step size of 0.005). It is observed that the peaks analogous to diffraction planes [111], [320], [311], [400], [511]

,[440] match with usual data of JCPDS card no. 022-1086 confirming FCC cubic spinel structure. The values of 'a' were calculated from the equation given below [9, 10, 11]

$$a= d *(h^2+k^2+l^2)^{1/2}$$

where cell constant is given by 'a', inter planer spacing calculated from Bragg's equation ($2\,d\sin\theta = n\lambda$) is denoted by 'd' and miller indices are denoted by 'h,k,l'. It was reported that, low concentration RE (rare earth) doping in spinel ferrite exhibit phase separation and grain boundary diffusion giving rise to precipitation of additional crystalline phases like hematite (a-Fe_2O_3), metal monoxides and orthoferrites ($REFeO_3$) [12,13, 14]. Hence in case of rare earth doped ferrites, Er^{+3}doped CFO having no impurity phase ($x\leq0.010$) is an exception which is due to auto-combustion. Induced effect due to substitution of erbium on the structure reflects two main observations given by decrease in size of crystal and increase in lattice constant both on small scale. The values of lattice constant increases with increased composition between x=0.000 to 0.030 . Scherrer formula was used to calculate the crystallite size given by

$$L=\frac{0.9*\lambda}{\beta cos\theta}(2)$$

where 'λ' = wavelength of X-ray,'β'= peak width at half maximum height and constant 'K'=0.9. The data related to intense peak (311) was used in estimating the size (L). The results indicated reduction in size of crystallite from 20.84 nmto14.40 nm (x=0.0 to 0.030). The values of lattice parameter, crystal size, X-ray density and surface area has been displayed in Table.1. It can be seen from the table that lattice parameter increases with increase in erbium content. This increase is due to replacement of eight small Co^{2+} and Fe^{3+} ions with big Er^{3+} ions. Huge difference in radii of these three ions induce strain during lattice formation and diffusion processes. Requirement of more energy in absorbing RE^{3+} ions with more radii while replacing Fe^{3+} to form RE-O bond decreases crystallization energy leading to particles of small size. Earlier reports indicated similar results on RE-ion substituted cobalt ferrites[15-20]. Therefore, XRD results are

liable for expansion of unit cell due to larger Er^{3+} ion doping in CFO. Calculation of X-ray density (Dx) was done using the equation [21]

$$d_x = \frac{8*M}{Na3} (3)$$

where 'M'= composition molecular weight, 'N'= Avogadro's number,'a'= lattice constant.

X-ray density is found to increase from 5.3344gm/cm^3 to 5.3392gm/cm^3 (x = 0.00 to x =0.030) with increasing Er^{3+} content. Cobalt ferrite in inverse spinel form has tetrahedral site half occupied by Fe^{+3} and octahedral sites occupied by remaining half of $Fe^{+3}$and Co^{-2} ions [22,23]. Any change in site occupation by Fe^{+3} and Co^{-2} ions might be due to preparation technique and affect cell constant.

$$S = \frac{6000}{D*d} (6)$$

Here, S= area of surface, D= crystallite size, d=Bulk density

3.2. TEM Analysis:

Phase structure and morphology studies of the synthesized samples were taken up by using TEM analysis. Figure3. shows the TEM images and their respective SAED images with particle size distribution chart for all samples respectively. TEM and SAED images demonstrated spherical shape and low thickness for majority of the nanoparticles along with few elongated particles. TEM images confirmed well distanced particles for lower concentration of Er^{+3} ions and increase in Er^{+3} ion substitution leads to agglomeration of particles due to magnetic nano-particle interaction. TEM images indicated the particle size ranging between 16nm-24nm.

Conclusions:

Erbium substituted Co-Er nano-ferrites were synthesized and characterized. Significant induced effect of Erbium was observed on crystal structure and morphology. Crystal size decreased with increased Erbium content. Study of $CoEr_xFe_{2-x}O_4$ for compositions with cobalt content (x=0.0 to 0.030) indicated decrease in crystallite size with increasing erbium content and increased particle surface area making it suitable for a good adsorbent. Hence these adsorbents can be used in gas sensors and waste water treatment.

Acknowledgments:

The authors acknwowledge Prof. Syed Rahman, HOD-Physics, Osmania University for his encouragement. Author **Edapalli Sumalatha** acknowledges CSIR, New Delhi, India for Research Fellowship (CSIR-JRF). Author KM Batoo acknowledges the Deanship of Scientific Research at King Saud University for financial support through the project (RG-1437-030).

References:

[1]. Q. Song and Z. J. Zhang, *J. Am. Chem. Soc.* 2004, 126, 19, 6164–6168, Publication Date:April 23, 2004, https://doi.org/10.1021/ja049931r
[2]. Maria A. G. Soler, Emilia C. D. Lima, Sebastião, *Langmuir* 2007, 23, 19, 9611–9617,Publication Date:August 16, 2007,https://doi.org/10.1021/la701358g
[3]. C. Vazquez-Vazquez, First published: 29 May 2008, https://doi.org/10.1002/pssa.200778128
[4].A.H.Habib, Journal of Applied Physics 103, 07A307 (2008); https://doi.org/10.1063/1.2830975
[5]. I. C. Nlebedim, Journal of Applied Physics 113, 17A928(2013); https://doi.org/10.1063/1.4798822
[6]. B. D. Cullity and C. D. Graham, Introduction to Magnetic Materials (Wiley/IEEE, NJ, 2009), https://www.wiley.com/en-in/Introduction+to+Magnetic+Materials%2C+2nd+Edition-p-9780471477419.
[7]. D. J. Craik (Ed.), Magnetic Oxides, Parts 1 and 2 (John Wiley & Sons, Bristol, 1975), Chap. 9, Pt. 2. 8, https://doi.org/10.1002/bbpc.19760800218
[8]. S. Prathapani, M.Vinita, T. V. Jayaraman and D. Das, Structural and ambient/sub-ambient temperature magnetic properties of Er-substituted cobalt-ferrites synthesized by sol-gel assisted auto-combustion method, Journal of Applied Physics 116, 023908 (2014); https://doi.org/10.1063/1.4889929
[9]. Heiba ZK, Bakr Mohamed M, Arda L, Dogan N. "Cation distribution correlated with magnetic properties of nanocrystalline gadolinium substituted nickel ferrite", https://doi.org/10.1016/j.jmmm.2015.05.003
[10]. Kambale PASRC, Kamble SS, Kolekar YD. Effect of cobalt substitution on structural, magnetic and electric properties of nickel ferrite.DOI**:** 10.4236/anp.2016.51012 .
[11]. B.D. Cullity, Elements of X-ray Diffraction, Addison-Wesley, London, 1959, Chap. 1-5, Pt. 2. 5, https://link.springer.com/chapter/10.1007/978-1-4613-4490-2_8.
[12]. Andreu, E. Natividad, C. Ravagli, M. Castro and G. Baldi, Heating ability of cobalt ferritenanoparticles showing dynamic and interaction effects, https://doi.org/10.1039/C4RA02586E.
[13]. S. G. Kakade, Y. R. Ma, R. S. Devan, Y. D. Kolekar, and C. V. Ramana, Dielectric, Complex Impedance, and Electrical Transport Properties of Erbium (Er3+) Ion-Substituted Nanocrystalline Cobalt-Rich Ferrite, (Co1.1Fe1.9−xErxO4), J. Phys .Chem. C, (2016). DOI: 10.1021/acs.jpcc.5b11188.
[14]. R. C. Kambale, K. M. Song, Y. S. Koo and N. Hur, Low temperature synthesis of nanocrystalline Dy doped cobalt ferrite: Structural and magnetic properties, Journal of Applied Physics **110**, 053910 (2011); https://doi.org/10.1063/1.3632987.

[15]. Hemaunt Kumar, Jitendra Pal Singh, R. C. Srivastava,P. Negi, H. M. Agrawal and K. Asokan, FTIR and electrical study of dysprosium dopedcobalt ferrite nanoparticles,https://doi.org/10.1155/2014/862415.
[16]. Mohd. Hashim a,*, Alimuddin a , Shalendra Kumar b , Sagar E. Shirsath c , R.K. Kotnala d , Jyoti Shah d , Ravi Kumar "synthesis and characterization of nickel substuded cobalt ferrite", https://doi.org/10.1016/j.matchemphys.2012.09.019
[17].A. B.Salunke, V.M.Khot, M.R.Padatare, N.D.Thorat,R.S.Joshi,H.M.Yadav and S.H. Pawar,"Low temperature combustion synthesis and magnetostructural properties of CoMnnano-ferrites",https://doi.org/10.1016/j.jmmm.2013.09.020.
[18]. S. R.Naik and A. V.Salker, Change in the magneto structural properties of rare earth doped cobalt ferrites relative to the magnetic anisotropy,https://doi.org/10.1039/C2JM15228B.
[19]. S. Prathapani, M.Vinita, T. V. Jayaraman and D. Das, Structural and ambient/sub-ambient temperature magnetic properties of Er-substituted cobalt-ferrites synthesized by sol-gel assisted auto-combustion method,https://doi.org/10.1063/1.4889929.
[20]. DeepshikhaRathore, RajnishKurchania, and R. K. Pande, Influence of particle size and temperature on the dielectric properties of CoFe2O4 nanoparticles, Int. J. Miner. Metall. Mater.21(2014) 409, https://doi.org/10.1016/j.jpcs.2016.03.015
[21]. P. Kumar, J. Chand , S. Verma and M. Singh , Journal of Applied Physics 116, 164108 (2014); https://doi.org/10.1063/1.4896945
[22]. Goldman, Modern Ferrite Technology, 2nd ed. (Springer Science, Business Media Inc., 2006), Chap.1-3, Pt. 3. 1,https://download.e-bookshelf.de/download/0000/0009/50/L-G-0000000950-0002340313.pdf.
[23]. M. Raghasudha, D. Ravinder, and P. Veerasomaiah, "FTIR Studies and Dielectric Properties of Cr Substituted Cobalt Nano Ferrites Synthesized by Citrate-Gel Method," DOI: 10.5923/j.nn.20130305.01

Compositions	Cell Constant Å	Crystallite Size (nm)	X-ray density(dx) (gcm−3)	Surface area(s) m^2/gm
$CoFe_2O_4$	8.361	20.84	5.3344	89.61
$CoEr_{0.005}Fe_{1.995}O_4$	8.367	20.43	5.3356	91.39
$CoEr_{0.010}Fe_{1.990}O_4$	8.373	19.19	5.3367	97.34
$CoEr_{0.015}Fe_{1.985}O_4$	8.379	19.02	5.3379	98.18
$CoEr_{0.020}Fe_{1.980}O_4$	8.386	17.73	5.3370	105.38
$CoEr_{0.025}Fe_{1.975}O_4$	8.392	15.56	5.3381	119.99
$CoEr_{0.030}Fe_{1.970}O_4$	8.398	14.40	5.3392	132.58

Table.1: Values of lattice constant, Crystal Size, X-Ray density and Surface area.

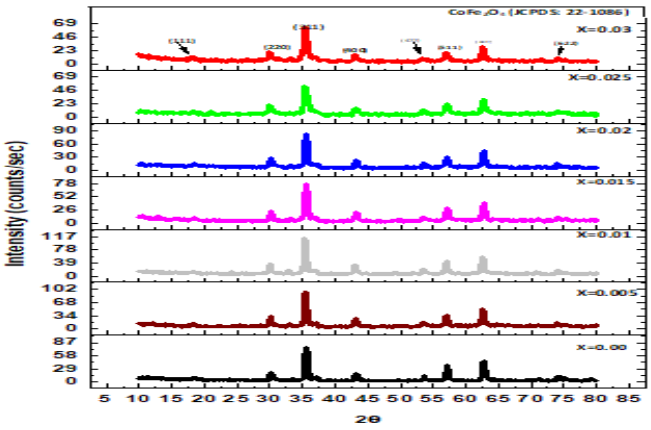

Fig. 1. XRD patterns for $CoEr_xFe_{2-x}O_4$nano-ferrites

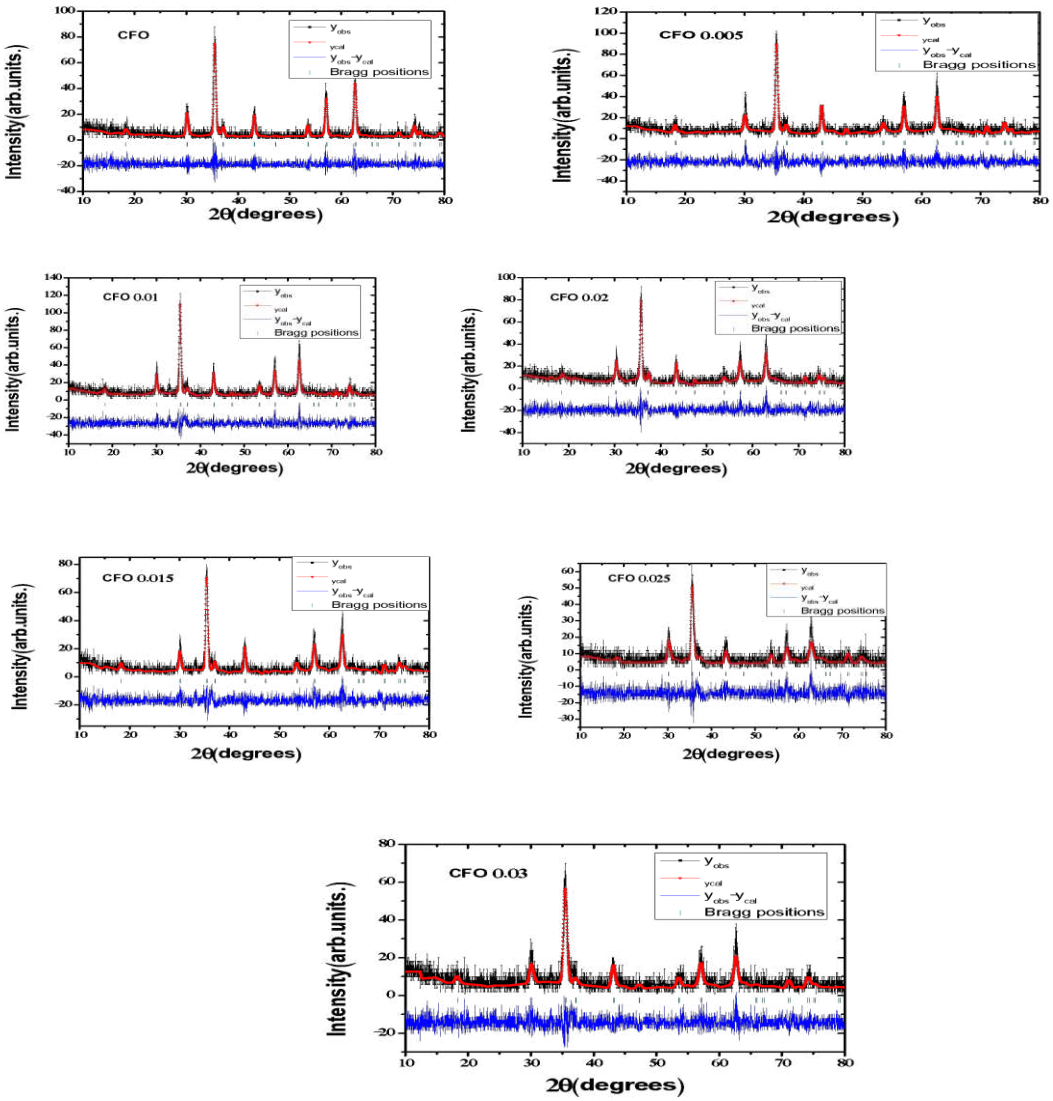

Fig. 2. Rietveld Refinement of $CoEr_xFe_{2-x}O_4$nano-ferrites.

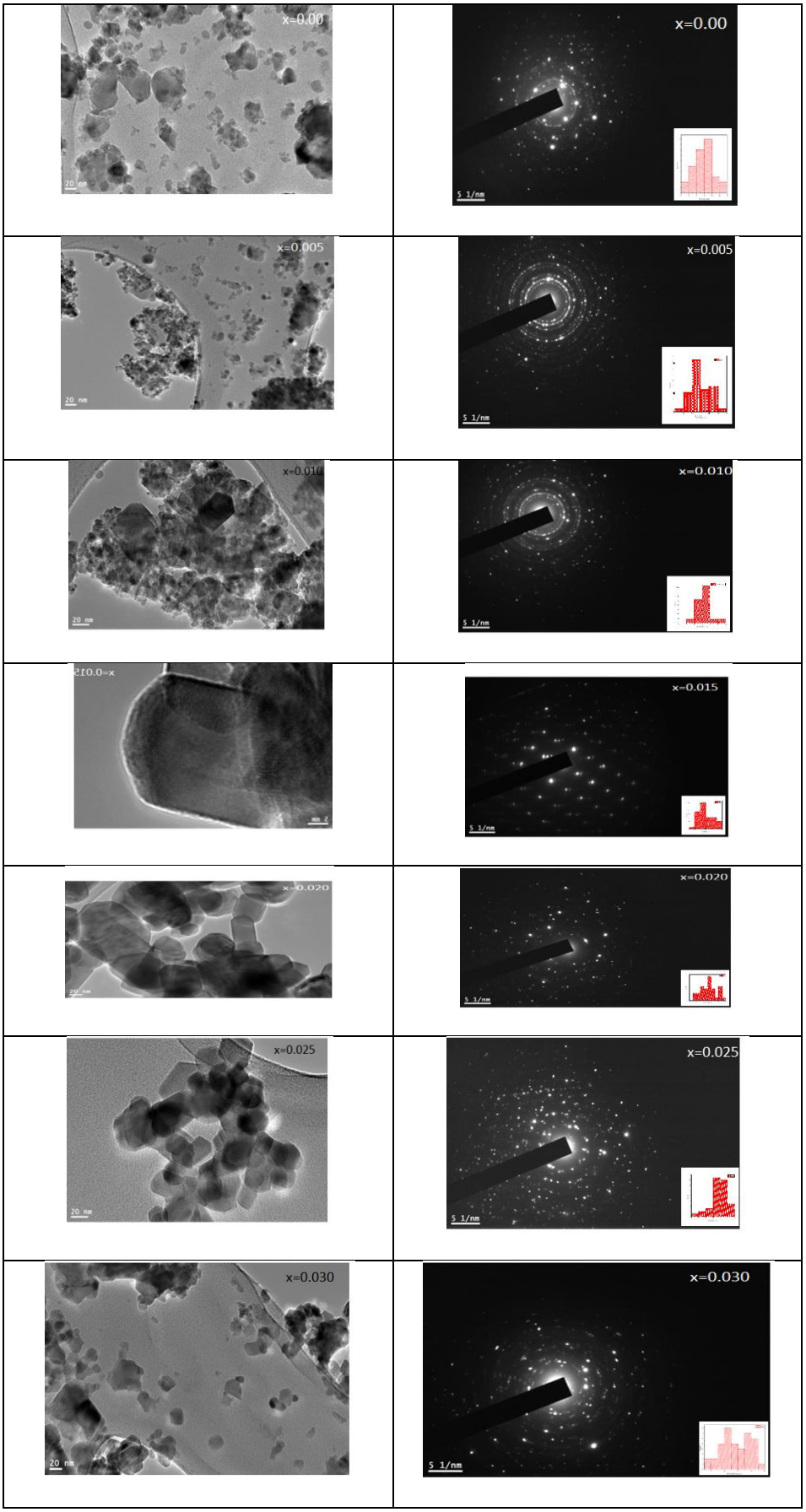

Fig.3: FE-TEM with SAED images

Figures

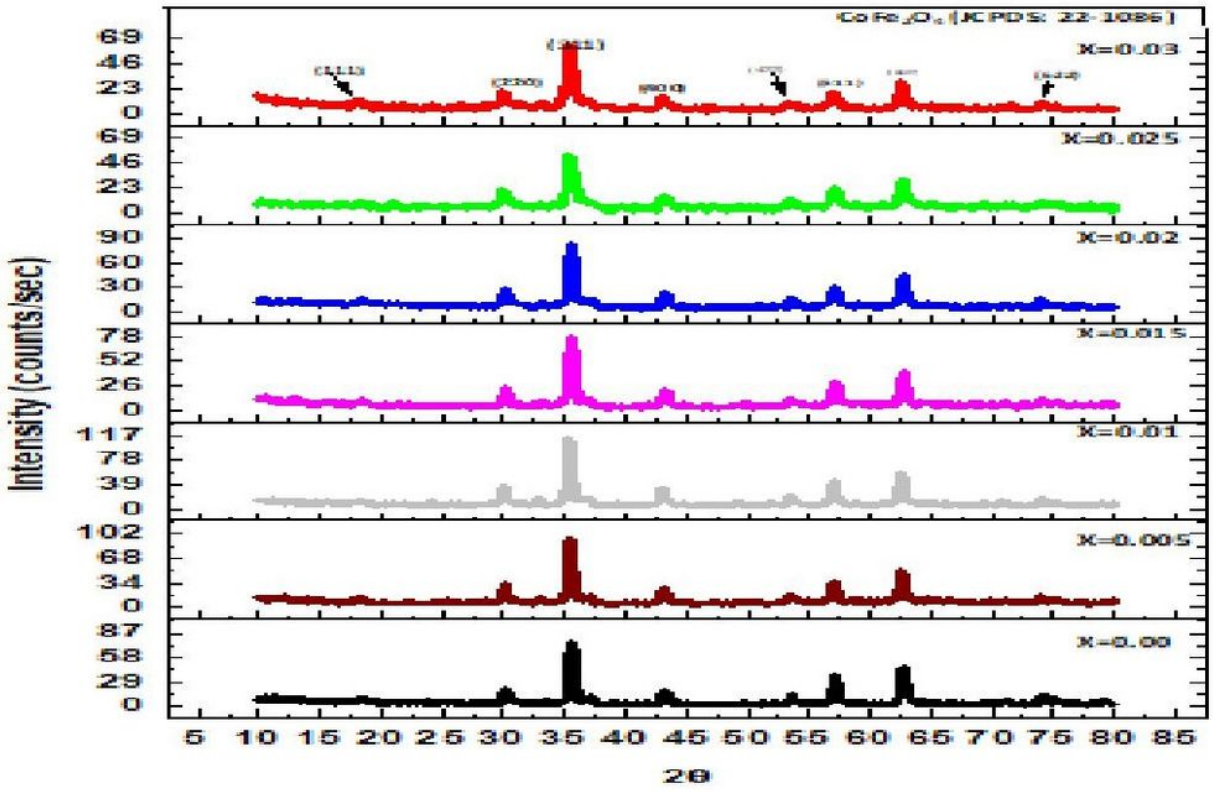

Figure 1

XRD patterns for CoErxFe2-xO4nano-ferrites

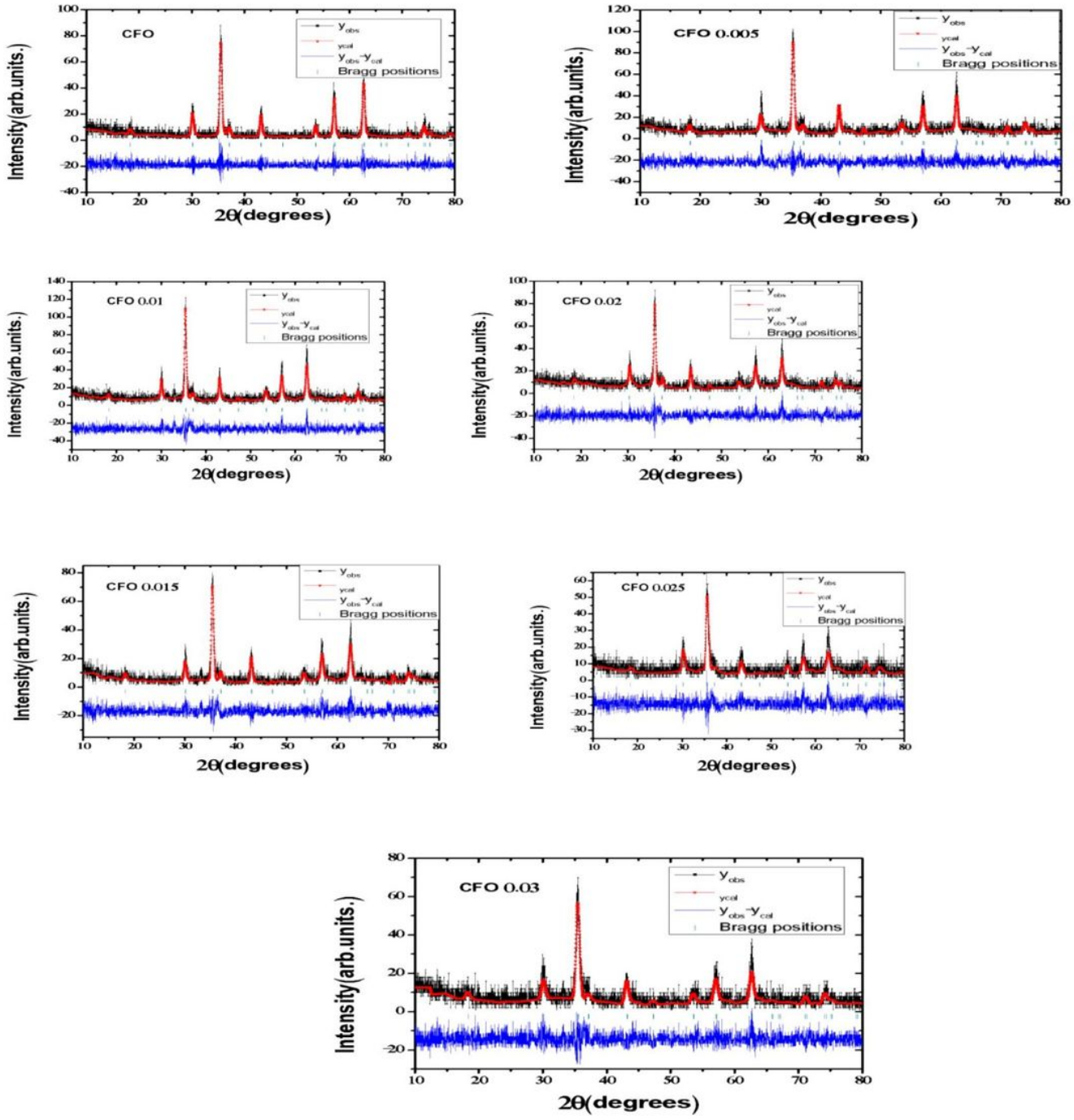

Figure 2

Rietveld Refinement of CoErxFe2-xO4nano-ferrites.

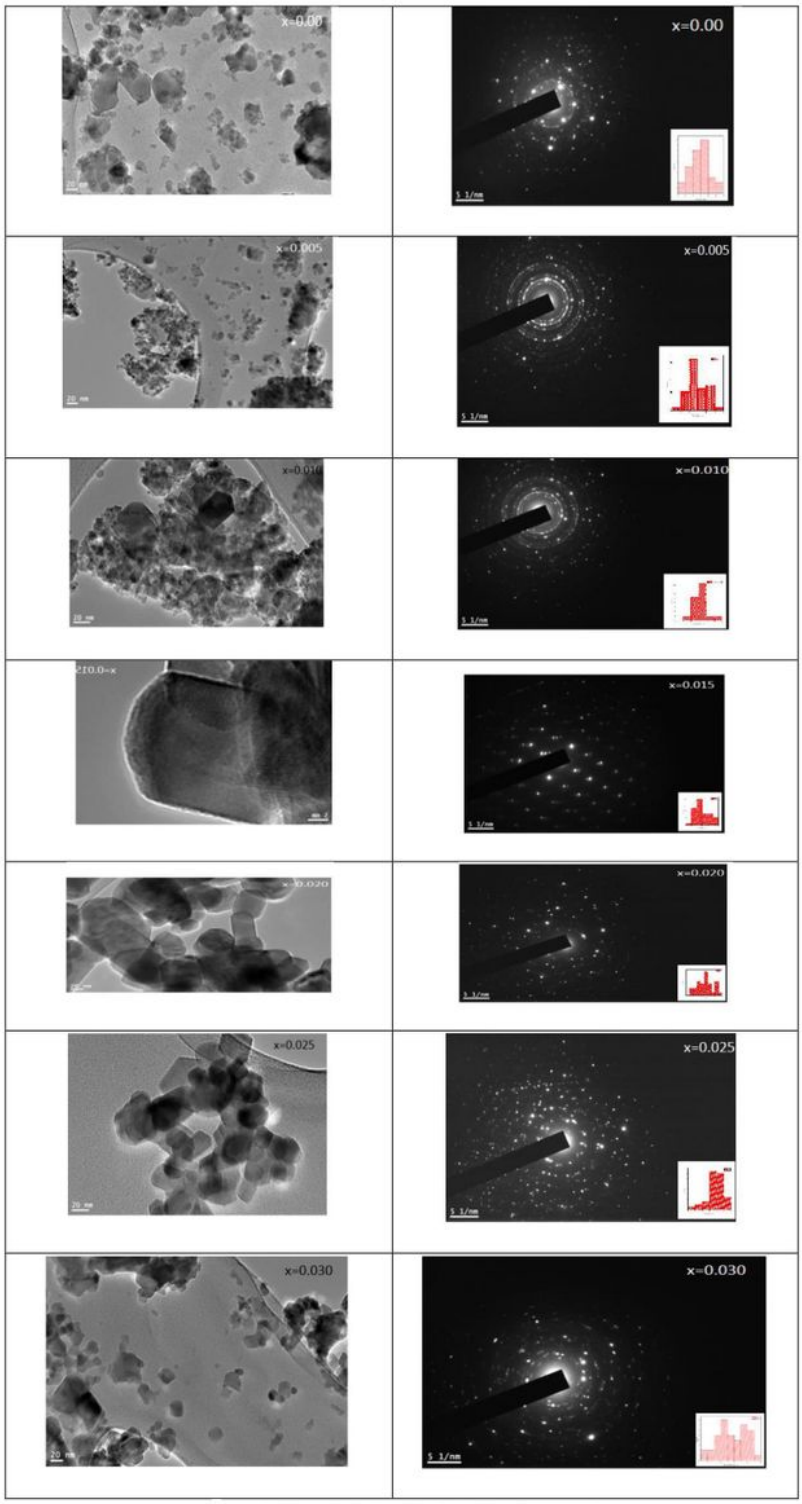

Figure 3

FE-TEM with SAED images